Effect of working fluids on the performance of a novel direct vapor generation solar organic Rankine cycle system

Jing Li[1], Jahan Zeb Alvi[1], Gang Pei[1*], Jie Ji[1], Pengcheng Li[1], Huide Fu[2]

[1]Department of Thermal Science and Energy Engineering, University of Science and Technology of China, 96 Jinzhai Road ,Hefei, China

[2]Department of Energy and Environmental Engineering, Shenzhen University, 3688 Nanhai Road, Shenzhen, China

**Corresponding author. Tel: +86 551 63607367. E-mail:* peigang@ustc.edu.cn

Abstract: A novel solar organic Rankine cycle (ORC) system with direct vapor generation (DVG) is proposed. A heat storage unit is embedded in the ORC to guarantee the stability of power generation. Compared with conventional solar ORCs, the proposed system avoids the secondary heat transfer intermediate and shows good reaction to the fluctuation of solar radiation. The technical feasibility of the system is discussed. Performance is analyzed by using 17 dry and isentropic working fluids. Fluid effects on the efficiencies of ORC, collectors and the whole system are studied. The results indicate that the collector efficiency generally decreases while the ORC and system efficiencies increase with the increment in fluid critical temperature. At evaporation temperature of 120^{o}C and solar radiation of 800 Wm^{-2}, the ORC, collector and overall thermal efficiencies of R236fa are 10.59, 56.14 and 5.08% while their values for Benzene are 12.5, 52.58 and 6.57 % respectively. The difference between collector efficiencies using R236fa and Benzene gets larger at lower solar radiation. The heat collection is strongly

correlated with latent and sensible heat of the working fluid. Among the fluids, R123 exhibits the highest overall performance and seems to be suitable for the proposed system in the short term.

Keywords: *solar thermal power generation, organic Rankine cycle, direct vapor generation, working fluid, critical temperature*

1. Introduction

Solar energy is one of the potential heat source for organic Rankine cycle (ORC). Solar radiation has the maximum capacity and the minimum replenishment time among all of available sustainable energies [1]. By using the ORC, low-medium temperature solar thermal power system can be an attractive option. A temperature of about 100°C or slightly higher is sufficient to drive the ORC and evacuated/double glazing flat plate collectors (FPC), evacuated tube collectors (ETC), compound parabolic concentrators (CPC), and parabolic trough collectors (PTC) with small concentration ratio can be competent in solar energy collection for the ORC. Such solar ORC systems are capable to efficiently harness solar energy in temperature ranges from 100 to 200°C. They have advantages including the ability to scale down to small unit sizes, cogeneration near the point of usage, relatively low technical requirement in heat storage and good applicability in regions without rich direct solar radiation resource.

At present, most of the solar ORCs under investigation use heat transfer fluid (HTF) to carry away energy in the collectors and then release it to the organic fluid [2-11]. The heat transfer irreversibility in the evaporator is very large as shown in Fig. 1. The vertical axis is the temperature and the horizontal is the heat transferred from HTF to the organic fluid. Adverse current heat exchanger is exemplified. The inlet temperature of the organic fluid is close to the environment temperature. Given the pinch point temperature (ΔT_{pp}) and the ORC operating condition, a low mass flow rate of HTF results in a high HTF inlet temperature while a high one

is accompanied with a high HTF outlet temperature. Therefore, it is difficult to lower the HTF average temperature. This is disadvantageous because solar energy collection is less efficient at high operating temperature. Moreover, the use of HTF increases the investment. Additional power is needed for the pumping of HTF, which can significantly reduce the system net power output especially for small-scale solar ORCs.

The above mentioned problems can be solved by using direct vapor generation (DVG) technology. The DVG technology with water as the working fluid (known as direct steam generation, DSG) has been widely investigated [12-16]. In a DSG system, steam is directly generated in the solar field, hence eliminating the boiler in the power section. The power consumption by the solar field recirculating pump is also reduced. The collectors benefit from the constant temperature and high coefficient of heat transfer in the evaporation region of water. The feasibility of the DSG technology has been demonstrated within the DISS (Direct Solar Steam) project [17, 18]. During the 1500 hours operation no problem in the solar specific components like the absorber tubes or the ball joints has occurred. A demonstration plant of 8 MWht has also been built by Abengoa Solar [19]. The plant has been operated and evaluated for one year. In this period, an innovative control strategy system that guarantees the stability of the plant even under transient conditions has been validated. The first commercial solar thermal parabolic trough power plant with DSG technology in the world has been producing electricity since 2011 [20]. The 5 MWe solar thermal power plant uses a new generation of parabolic trough made of composite material combined with an efficient thin-glass mirror which reflects more than 95% of the sun radiation. After two years of successful operation, the power plant has shown practical applicability of the DSG technology.

Though the DVG technology using the organic fluid for the purpose of power conversion has not yet attracted much attention, it seems to be a perfect match to the ORC. The reasons are given as follows.

Firstly, it can react to the fluctuation in solar radiation in a simple way. In the conventional DSG power generation system, in order to prevent the droplets from hitting the blades and causing damage, the water (a typical wet fluid) entering the expander must be superheated. This leads to great difficulty in controlling the system under variable solar radiation. The superheated steam is also accompanied by low coefficient of heat transfer in the receiver, and thus the collector efficiency is decreased. Through the replacement of water by a dry or isentropic organic fluid, these problems can be overcome. There is no need to guarantee the superheat state when the fluid leaves the solar field. The fluid from the collectors can be even at liquid or binary phase state with a specially designed heat storage unit. The power generation is steady over a wide range of solar radiation, which is certainly a big advantage of this kind of system.

Secondly, the technical issues associated with the pressure are less critical. In the conventional DSG system, the maximum operation pressure is generally above 10 MPa, and the technical requirement on the receiver is high. While in a DVG-ORC system the pressure can be significantly reduced by choosing appropriate fluids. For example, the saturation pressure of R245fa at 100 ºC is 1.3MPa, and it is 1.3 MPa for R123 at 125 ºC, 1.1 MPa for Acetone at 150 ºC, 1.6 MPa for PF5056 (Perfluorohexane) at 175 ºC, 1.3 MPa for Cyclohexane at 200 ºC. These fluids can be considered for different operating temperatures. The technical requirement in the DVG system gets much lower than that in the DSG system. Moreover, the operating pressure in the DVG system may be even lower than that of HTF in a commercial solar thermal power plant. The mixture of two aromatic hydrocarbons (diphenyl and diphenyl ether, THERMINOL® VP-1)

is suitable fluid to transport heat in the solar field [21, 22]. The saturation pressure of this HTF at 400ºC is about 1.2 MPa. The design pressure at the solar field inlet has been set at 2.5 MPa to avoid evaporation at the outlet of the solar field. The technical issues associated with the HTF pressure in the receiver, storage tank, etc. are similar with those in the DVG system. Since the HTF technology has been well proven, the DVG technology is expected to be feasible.

Thirdly, there have been many successful applications of DVG technology using refrigerant. One application is the solar assisted heat pump (SAHP) systems [23-26]. CPC, FPC and evacuated heat pipe collectors can be employed. The solar collectors and the heat pump evaporator are integrated into a single unit to transfer solar heat to the refrigerant. The direct expansion SAHP systems are widely used for domestic heating and bathing. Long-term performance (>5years) has been investigated and demonstrated [27]. There are products available in the market [28, 29]. R134a is a commonly used fluid in SAHP systems, in which the operating pressure may range from 0.4 to 1.6 MPa (the saturation pressure at 10 and 60 ºC respectively). The DVG technology with low boiling point refrigerant has reached a considerable degree of maturity.

The solar ORC system with DVG is promising. However, study on this kind of system is limited. A close view to its performance is required. In particular, as vapor is generated directly in the collectors, the working fluid influences not only the heat to power conversion but also the solar energy collection. Among the properties of the working fluid, the critical temperature seems to be most relevant to the thermodynamic performance. The effects of fluid critical temperature on the efficiencies of isolated ORC [30-32], geothermal power generation [33], waste heat recovery [31, 34, 35] and solar power system [3] have been estimated by lots of

researchers. A general conclusion has been made: higher system efficiency can be achieved by using fluid of higher critical temperature.

Notably, the influence of working fluids on the solar energy collection is rarely investigated. In the proposed solar ORC system, an inner-type heat storage unit is employed, which enables the system to work steadily. Seventeen fluids have been selected as listed in Table 1. These working fluids have also been examined in many previous studies [3, 7, 31, 32, 36]. The working fluids are vaporized directly in the collectors. Due this innovative design the effect of working fluids is different from that on a solo ORC or conventional solar ORC system with HTF. In this paper, influence of working fluids on the collectors, ORC, and the whole system is investigated with respect to their critical temperatures. Suitable fluids are suggested with comprehensive consideration of the thermodynamic efficiency, technical and environmental aspects.

2. System configuration

The configuration of the proposed system is shown in Fig. 2. The system consists of solar collectors, pumps (P) and a fluid storage tank with phase change material (PCM), expander, generator (G) and condenser. The collectors serve as the direct vapor generator. In contrast to the traditional solar Rankine system, an organic fluid storage tank with PCM is embedded into the system. Owing to this inner-type heat storage unit, the system can work smoothly without any complicated control strategy.

In practical operation, there can be three modes:

Ⅰ) The system needs to generate electricity and solar radiation is available. In this mode, valves 1, 2 and 3 are open and pump 1 is running. The organic fluid is heated and vaporized through the collectors under high pressure. The vapor flows into the expander, exporting power in the process due to the pressure drop. The outlet vapor is cooled down and condensed to a liquid state

in the condenser. The liquid is pressurized by pump 1. The organic fluid is then sent back to the collectors for recirculation. In case solar radiation is too strong (higher than the design value), valve 4 can be open and pump 2 can run to prevent the organic fluid from being superheated in the collectors and to efficiently utilize solar energy. Part of the solar heat is stored. If solar radiation is lower than the design value, some liquid can be vaporized by the PCM. The fluid leaving the collectors can be at vapor phase, binary phase or liquid phase, and the ORC is able to work steadily over a wide range of solar radiation.

Ⅱ) The system does not need to generate electricity but solar radiation is strong. Valves 3 and 4 are open. Pump 2 is running. In this mode, solar heat is transferred to the PCM by the organic fluid. Heat is stored.

Ⅲ) The system needs to generate electricity but solar radiation is very weak or unavailable. Valves 1, 2 and 5 are open and pump 1 is running. Heat is released from the PCM and converted into power by the ORC.

Mode Ⅰ presents the simultaneous processes of heat collection and power generation while Mode Ⅱ or Mode Ⅲ is the independent process of heat collection or power conversion.

3. Thermodynamic modelling

The power generated by the expander and that consumed by the pump are calculated by Eq. (1) and Eq. (2), respectively.

$$W_t = m(h_{t,i} - h_{t,o}) \tag{1}$$

$$W_p = m(h_{p,o} - h_{p,i}) \tag{2}$$

The isentropic efficiency for the expander and the pump is defined by Eq. (3) and Eq. (4),

$$\varepsilon_t = \frac{h_{t,i} - h_{t,o}}{h_{t,i} - h_{t,os}} \tag{3}$$

$$\varepsilon_p = \frac{h_{p,os} - h_{p,i}}{h_{p,o} - h_{p,i}} \tag{4}$$

where *os* represents the ideal thermodynamic process. The energy required in the heating process of the ORC is calculated by the enthalpy increment of the organic fluid from the pump to the expander.

$$Q = m(h_{t,i} - h_{p,o}) \tag{5}$$

The ORC efficiency is defined by the ratio of the net power output to the heat supplied,

$$\eta_{ORC} = \frac{W_t \cdot \varepsilon_g - W_p}{Q} \tag{6}$$

For the solar ORC system with DVG, the thermal efficiency of a solar collector is generally expressed by

$$\eta_{cl}(T) = \eta_{cl,0} - \frac{A}{G}(T - T_a) - \frac{B}{G}(T - T_a)^2 \tag{7}$$

The solar collector modules available on the market have effective area between 1.0 m^2 and 2.0 m^2 . Their thermal efficiency can be calculated by Eq. (7). In a solar ORC system tens or hundreds square meters of collectors are usually required, the temperature difference between neighboring collectors is supposed to be small. To calculate the overall collector efficiency it is reasonable to make the assumption that the average operating temperature of the collector changes continuously from one module to another. The working fluid in the collector is mostly at liquid-phase and binary phase. For the binary phase region, the temperature is constant and it is easy to calculate the collector efficiency. For the liquid phase region, in order to reach an outlet temperature T_o of the fluid with an inlet temperature T_i, the required collector area is obtained by

$$S_l = \int_{T_i}^{T_o} \frac{mC_p(T)}{\eta_{cl}(T)G} dT \tag{8}$$

177 The heat capacity of a fluid at liquid state can be expressed by a first order approximation

178 $$C_p(T) = C_{p,0} + \alpha(T - T_0) \tag{9}$$

179 With $c_1 = A/G$, $c_2 = B/G$, the collector area according to Eqs. (7), (8) and (9) is calculated by

180 $$S_l = \frac{m}{c_2 G(\theta_2 - \theta_1)}\left[(C_{p,a} + \alpha\theta_1)\ln\frac{T_o - T_a - \theta_1}{T_i - T_a - \theta_1} + (C_{p,a} + \alpha\theta_2)\ln\frac{\theta_2 - T_i + T_a}{\theta_2 - T_o + T_a}\right] \tag{10}$$

181 θ_1 and θ_2 are the arithmetical solutions of Eq. (11)（$\theta_1 < 0,\ \theta_2 > 0$）.

182 $$\eta_{cl,o} - c_1\theta - c_2\theta^2 = 0 \tag{11}$$

183 $$C_{p,a} = C_{p,0} + \alpha(T_a - T_0) \tag{12}$$

184 The thermal efficiency of the collectors with liquid is calculated by

185 $$\eta_{cl,l} = \frac{m(h_{l,o} - h_{l,i})}{GS_l} \tag{13}$$

186 The thermal efficiency of the collectors with working fluid in the binary-phase and the overall

187 collector system are calculated by Eq. (14) and Eq. (15), respectively,

188 $$\eta_{cl,b} = \frac{m(h_{b,o} - h_{b,i})}{GS_b} \tag{14}$$

189 $$\eta_{cl} = \frac{m(h_{b,o} - h_{l,i})}{G(S_l + S_b)} \tag{15}$$

190 The overall electricity efficiency of the solar ORC is expressed by

191 $$\eta_{sys} = \eta_{ORC} \cdot \eta_{cl} \tag{16}$$

192 The relative increment in overall electricity efficiency of solar ORC with DVG over that with

193 HTF is expressed by

194 $$\Delta\eta_{sys} = \frac{\eta_{sys,DVG} - \eta_{sys,HTF}}{\eta_{sys,HTF}} \tag{17}$$

195 **4. Results and discussion**

In this section the influence of working fluid on the system performance is evaluated with respect to the critical temperature. The effects of fluid critical temperature on the ORC efficiency at given evaporation temperature, on optimum evaporation temperature and maximum system efficiency at given solar radiation, on solar energy collection efficiency at given evaporation temperature and solar radiation, and on overall system efficiency at given evaporation temperature and solar radiation, are investigated successively. An efficiency comparison between the solar ORCs with DVG and HTF is conducted.

Some assumptions are made in the simulation: Evaporation and condensation processes are isobaric while expansion and pressurization processes are adiabatic. Pump, expander and generator efficiencies are 0.65, 0.75 and 0.85 respectively. The first heat loss coefficient A of solar collectors is 0.82 $Wm^{-2}°C^{-1}$, the second heat loss coefficient B is 0.0064$Wm^{-2}°C^{-2}$, and the optical efficiency is 0.661. These are common values for commercial medium temperature collectors [37].

4.1. Effect of critical temperature on ORC efficiency at given evaporation temperature

The ORC efficiency variation with the critical temperature of 17 different working fluids is shown in Fig. 3. At a given evaporation temperature, the ORC efficiency generally increases with increment in the critical temperature which is consistent with the previous results by Liu et al. [34] and Aljundi et al. [30]. As this study is limited to subcritical cycle, some fluids of relative low critical temperatures are excluded at higher evaporation temperature (120 and 150 ^{o}C).

It is observed that by increasing evaporation temperature, fluids of higher critical temperature result in more significant increment in ORC efficiency as compared to the lower critical temperature fluids. Therefore, the efficiency difference among the fluids is increased with the

219 increment in evaporation temperature. For instance, the ORC efficiency using benzene
220 overcomes that using butane by 14.36 % at evaporation temperature of 100^{o}C, while the value is
221 31.82 % at the evaporation temperature of 150^{o}C.

222 **4.2. Effect of critical temperature on optimum evaporation temperature and maximum**
223 **thermal efficiency at given solar radiation**

224 Optimum evaporation temperature is a useful parameter in system design. At a given solar
225 radiation, optimum evaporation temperature is the temperature at which maximum solar thermal
226 power efficiency is achieved. For each fluid, the optimum evaporation temperature is a
227 compromise between the efficiencies of solar energy collection and power conversion. The
228 increment in the evaporation temperature will lead to higher power conversion efficiency but
229 lower collector efficiency. Effect of critical temperature on optimum evaporation temperature at
230 four consecutive levels of radiation (400, 600, 800 and 1000Wm^{-2}) of 17 working fluids is shown
231 in Fig. 4.

232 At stronger solar radiation, the optimum evaporation temperature increases with the
233 increment in critical temperature for most working fluids but in case of weaker solar radiation it
234 becomes constant and even a decreasing trend can be found. The reason behind this phenomena
235 is that when the solar radiation decreases, fluids having higher critical temperature show very
236 large decrement in their optimum evaporation temperature as compared to fluids having lower
237 critical temperature. For example, if solar radiation decreases from 1000 to 400 Wm^{-2}, optimum
238 evaporation temperature of benzene is decreased by 57^{o}C while for R227ea it is decreased by
239 merely 2^{o}C. Notably, when the evaporation temperature gets close to the critical temperature of
240 a fluid, the ORC efficiency may increase very slowly or even decrease with increasing

241 evaporation temperature. This leads to a relatively constant optimum evaporation temperature
242 which is near the critical temperature of the fluid.

243 At solar radiation of 1000 Wm^{-2}, isopentane and R236ea have not shown optimum
244 evaporation temperatures within their critical temperature.

245 The maximum solar thermal power efficiencies of the 17 working fluids are shown in Fig. 5.
246 In general, maximum thermal efficiency at given solar radiation acts as an increasing function of
247 critical temperature.

248 The difference of maximum thermal power efficiency among the working fluids decreases
249 with the decrement in solar radiation. For instance, at 1000Wm^{-2} relative increment in maximum
250 thermal efficiency of benzene over R227ea is 63.87 %, while the value decreases to 33.55 % at
251 solar radiation of 400 Wm^{-2}. The reason is as the solar radiation gets weaker, fluids having
252 higher critical temperature show larger decrement in maximum thermal power efficiency in
253 comparison with fluids having lower critical temperature.

254 The variation in maximum thermal efficiency has not shown same trend as shown by ORC
255 efficiency. At the solar radiation of 400 Wm^{-2}, the optimum evaporation temperatures of all
256 fluids under consideration are around 105 ^{o}C. At this evaporation temperature, the relative
257 increment in maximum solar thermal power efficiency of benzene over RC318 is 27.69%, while
258 the relative increment in ORC efficiency of benzene over RC318 is 40.53%. The inconsistent
259 variations of maximum solar thermal power efficiency and ORC efficiency indicate that the
260 influence of working fluids on collector efficiency cannot be neglected.

261 **4.3. Effect of critical temperature on collector efficiency at given evaporation temperature**
262 **and solar radiation**

In a conventional solar ORC system with HTF, the collector efficiency depends on the heat transfer from the HTF to the organic fluid. For most collectors the efficiency drops faster at higher operation temperature. A large mass flow rate of HTF is generally preferable to reduce the peak temperature in the collectors and to achieve a high overall heat collection efficiency [22]. Given information on the heat transfer (e.g. the pinch point temperature of 10^{o}C, ratio of mass flow rates of HTF and organic fluid of 10), the effect of working fluid on collector efficiency will be not significant as shown in Fig. 6. The difference of collector efficiencies among the working fluids is very small. However, in the solar ORC system with DVG, effect of critical temperature on collector efficiency is much more appreciable. Some results are shown in Figs. 7, 8 and 9. Collector efficiency is calculated at three levels of evaporation temperature as well as on four stages of solar radiation. On the whole, at given evaporation temperature and solar radiation, collector efficiency is a decreasing function of critical temperature. It is concluded that in case of DVG system, critical temperature strongly affects collector efficiency which will further affect the electricity efficiency of the system.

Behind this phenomenon, it is found that fluids of higher critical temperature have usually higher value of enthalpy ratio (ratio of the latent of vaporization to the sensible heat) as shown in Fig. 10. The sensible heat is the amount of heat required to raise the temperature of working fluid from subcooled liquid to saturated liquid state, while latent heat of vaporization is the heat required to change phase of the fluid from saturated liquid to saturated vapor phase. Higher enthalpy ratio elevates the average operating temperature of the collectors which results in decrement in collector efficiency.

At a given evaporation temperature, difference of collector efficiencies among the working fluids increases with the decrement in solar radiation. This is because fluids having higher

critical temperature show larger decrement in their collector efficiency. For example, at evaporation temperature of 100^{o}C when solar radiation changes from 1000 to 400Wm^{-2}, the collector efficiency using benzene is decreased by 12.17 % while for R227ea it is decreased by 9.1%. So, the influence of critical temperature on collector efficiency becomes more significant at weaker solar radiation.

Furthermore, the influence of critical temperature on collector efficiency becomes more evident at higher evaporation temperature. At the evaporation temperature of 150^{o}C, when the solar radiation changes from 1000 to 400 Wm^{-2}, the collector efficiency using benzene is decreased by 27.18 %.

4.4. Effect of critical temperature on thermal efficiency of the system at given evaporation temperature and solar radiation

Effect of critical temperature on solar thermal power efficiency is shown in Figs. 11, 12 and 13. In general, thermal efficiency of the system is observed to be an increasing function of critical temperature. However, it becomes constant and even a decreasing trend could be found at weak solar radiation and high evaporation temperature. As shown in Fig. 13, the system thermal efficiency is decreased with the increment in critical temperature at evaporation temperature of 150^{o}C and solar radiation of 400 Wm^{-2}. At weaker solar radiation and higher evaporation temperature effect of critical temperature on collector efficiency gets more evident. Therefore, system thermal efficiency starts decreasing with the critical temperature on these conditions.

At a given evaporation temperature, difference of system thermal efficiencies among the working fluids decreases with the decrement in solar radiation. That is because fluids having higher critical temperature show larger decrement in the system thermal efficiency as compared to lower critical temperature fluids. At evaporation temperature of 100^{o}C, decrement in system

thermal efficiency of benzene is 1.86% if solar radiation decreases from 1000 to 400 Wm^{-2}, while for R227ea it is only 1.22%.

4.5. Efficiency comparison between solar ORCs with DVG and HTF

The proposed system is simpler than conventional solar ORCs due to the elimination of HTF. The irreversibility in the collectors can be reduced by the high coefficient of phase-change heat transfer. Besides, the solar ORC with DVG is more advantageous in terms of overall electricity efficiency, as shown in Table 2. The evaporation temperature is 120 ^{o}C. The solar radiation ranges from 400 to 1000 W/m^2. The pinch point temperature difference between HTF and organic fluid is 10 ^{o}C. The efficiency superiority of solar ORC with DVG is highly appreciable under low solar radiation. The relative increment in efficiency ($\Delta\eta_{sys}$) varies from about 8% to 50%, and fluids of lower critical temperature generally offer larger $\Delta\eta_{sys}$.

4.6 Suitable working fluids for the solar ORC with DVG

Thermodynamic efficiency is just one aspect of fluid for the solar ORC application. It is necessary to take into account other issues including toxicity, flammability, cost, availability, ODP and GWP [2]. The selection of working fluid in the proposed system is more crucial than that for solar ORCs with HTF. In light of the system characteristics, there are some criteria the working fluid should meet.

(1) Dry or isentropic fluid. At the present of a dry or isentropic fluid, optimum ORC performance can be achieved when fluid operates along the saturation vapor curve without being superheated [38-43]. On the other hand, wet fluids are not favorable in the ORCs. They are not desirable for the solar ORC system with DVG owing to the need of superheat at the inlet of the turbine to avoid droplets during expansion process [44]. This will lead to inefficient solar energy collection regarding the low conductivity of superheated vapor. For example, the conductivity of

R134a at 150 ºC and 2.0MPa (superheat) is only 0.025$Wm^{-1}K^{-1}$. Moreover, it is not easy to guarantee a superheat state of fluid under fluctuating solar radiation. The fluid storage tank with PCM is unable to function as a superheater. The system control strategy is complicated in order to prevent part load operation of the turbine.

(2) Moderate operation pressure. Compared with ORCs for utilization of industrial waste heat, geothermal energy and biomass energy, solar ORC with DVG is more susceptible to the operating pressure. The collectors and storage unit are expected to play a prominent role in the cost-effectiveness of the system. According to Fig.2, higher operating pressure leads to stricter technical requirement in the collectors and storage tank. Thicker pipe and tank are needed and the cost is increased. For the sake of low cost, fluids having operating pressure less than 2 MPa are preferred. 2 MPa is a pressure that many commercial solar collectors can tolerate [45].

(3) Proper critical temperature. Supercritical cycle is not suitable for the solar ORC system with DVG because, in practical operation, it is difficult to control the pressure and temperature of fluid leaving the collectors. The expander can also suffer from off-design operation. Conversely, subcritical cycle can offer constant temperature and pressure in the vaporization process. By employing an inner-type heat storage unit it is much easier to maintain a steady state of fluid at the inlet of the expander, as illustrated in Section 2. To obtain an acceptable power conversion efficiency, the hot side temperature of the solar ORC system is usually higher than 100^{o}C. Therefore, a critical temperature higher than 100^{o}C is required for the fluid.

The fluid selection is a cumbersome process since it is difficult for one fluid to meet all the criteria. Among the various fluids, R245fa is commonly investigated and numerous works on its performance can be found in the literature. This fluid has zero ODP and low GWP, and thus is considered to be a promising replacement for chlorine-containing compounds. It is also favorable

and recommended in commercial ORC plants [46-48]. However, R123 may be a more suitable fluid than R245fa for the proposed system in the short term regarding its lower operating pressure as well as higher efficiency. For example, the saturation pressure of R123 at 30 ^{o}C and 120 ^{o}C is 0.11 MPa and 1.20 MPa, while it 0.17 MPa and 1.93 MPa for R245fa. R123 is also more beneficial than benzene and cyclohexane in the temperature range below 120 ^{o}C, because it is not flammable and avoids inward leakage of air through the collectors more easily when solar radiation is unavailable. The saturation pressure of benzene and cyclohexane at 30 ^{o}C is only 15.9 kPa and 16.2kPa, and high vacuum can be facilitated especially in cold environment.

Under current legislation, R123 will be phased out by 2030 due to an ODP of 0.02. Fortunately, new fluids which exhibit similar thermodynamic performance as R123 but have more environmentally friendly properties, are being developed. HFO1336mzz(Z) (cis-$CF_3CH=CHCF_3$) is a representative. It is a dry fluid, and has zero ODP, very low GWP of 9 and extremely good thermal stability at temperature up to 250^{o}C [49]. Its boiling point is 33.4 ^{o}C and the saturation pressure at 120 ^{o}C is about 1.1 MPa [50]. It is deemed as drop-in replacement of R245fa and R123, and can be used in ORCs, high temperature heat pumps as well as air conditioning chillers [51]. So far studies on the performance of HFO1336mzz(Z) as an ORC fluid have been based on experimental data from DuPont. Comprehensive information about this fluid is unavailable on the database like REPROP and CoolProp, and its latent heat of vaporization has been predicted by molecular simulations [52]. In view of the operating pressure, toxicity, flammability, ODP and reported power efficiency [50], HFO1336mzz(Z) might be an alternative working fluid for the solar ORC with DVG in the long term.

5. Conclusions

377 The solar ORC system with DVG is feasible. It has much lower operating temperature and
378 pressure than solar thermal power generation system with DSG. Depending on the working fluid,
379 its operating pressure can be even lower than that of HTF in recent commercial solar thermal
380 power plants. The commercialization of DVG technology in the SAHP application highlights the
381 potential of the proposed system. With the inner-type heat storage unit, the system can generate
382 power smoothly. Compared to conventional solar ORC systems, the proposed system excludes a
383 secondary heat transfer circuit, and the heat transfer irreversibility and negative power for pumps
384 are reduced. The efficiency increment of solar ORC with DVG over that with HTF is very
385 significant. All these advantages make the proposed system suitable for distributed power
386 generation.

387 The effect of working fluids on the system performance is analyzed. Isentropic and dry fluids
388 of moderate critical pressure and proper critical temperature are good match to the DVG.
389 According to the simulation results, the working fluid of solar ORC system with DVG affects
390 significantly the heat collection efficiency. In contrast to the ORC efficiency, the collector
391 efficiency generally decreases with the increment in the fluid critical temperature. At lower solar
392 radiation, the effect of fluid critical temperature on the collector efficiency is more significant
393 while the effect on optimum evaporation temperature is less appreciable.

394 Working fluid selection is crucial to the solar ORC with DVG. The system cost is supposed
395 to be strongly related to the operating pressure. R123 seems preferable to R245fa in light of
396 operating pressure and the efficiency, and can be employed for the DVG system in the short term.
397 The former has an overall electricity efficiency of about 6.1% on the condition of evaporation
398 temperature of 120 ^{o}C and solar radiation of 800W/m^{2}.

399

Acknowledgment

This study was sponsored by the National Science Foundation of China (51476159, 51378483, 51206154, 51178442), CAS-TWAS presidential fellowship program, Fundamental Research Funds for the Central Universities of China, Dongguan Innovative Research Team Program (2014607101008), and the Key Laboratory of New Lithium-ion Battery and Mesoporous Material.

References

1. Hermann, W.A., *Quantifying global exergy resources.* Energy, 2006. 31(12): p. 1685-1702.
2. Delgado-Torres, A.M. and L. García-Rodríguez, *Analysis and optimization of the low-temperature solar organic Rankine cycle (ORC).* Energy Conversion and Management, 2010. 51(12): p. 2846-2856.
3. Rayegan, R. and Y.X. Tao, *A procedure to select working fluids for Solar Organic Rankine Cycles (ORCs).* Renewable Energy, 2011. 36(2): p. 659-670.
4. Delgado-Torres, A.M. and L. García-Rodríguez, *Design recommendations for solar organic Rankine cycle (ORC)–powered reverse osmosis (RO) desalination.* Renewable and Sustainable Energy Reviews, 2012. 16(1): p. 44-53.
5. Kosmadakis, G., et al., *Economic assessment of a two-stage solar organic Rankine cycle for reverse osmosis desalination.* Renewable Energy, 2009. 34(6): p. 1579-1586.
6. Tchanche, B.F., et al., *Exergy analysis of micro-organic Rankine power cycles for a small scale solar driven reverse osmosis desalination system.* Applied Energy, 2010. 87(4): p. 1295-1306.

7. Tchanche, B.F., et al., *Fluid selection for a low-temperature solar organic Rankine cycle.* Applied Thermal Engineering, 2009. 29(11): p. 2468-2476.
8. Wang, J., et al., *Off-design performance analysis of a solar-powered organic Rankine cycle.* Energy Conversion and Management, 2014. 80(0): p. 150-157.
9. Manolakos, D., et al., *On site experimental evaluation of a low-temperature solar organic Rankine cycle system for RO desalination.* Solar Energy, 2009. 83(5): p. 646-656.
10. Quoilin, S., et al., *Performance and design optimization of a low-cost solar organic Rankine cycle for remote power generation.* Solar Energy, 2011. 85(5): p. 955-966.
11. He, Y.-L., et al., *Simulation of the parabolic trough solar energy generation system with Organic Rankine Cycle.* Applied Energy, 2012. 97(0): p. 630-641.
12. Birnbaum, J., et al., *A direct steam generation solar power plant with integrated thermal storage.* Journal of Solar Energy Engineering, 2010. 132(3): p. 031014.
13. Laing, D., et al., *Thermal energy storage for direct steam generation.* Solar Energy, 2011. 85(4): p. 627-633.
14. Montes, M., et al., *Performance analysis of an integrated solar combined cycle using direct steam generation in parabolic trough collectors.* Applied Energy, 2011. 88(9): p. 3228-3238.
15. Eck, M. and T. Hirsch, *Dynamics and control of parabolic trough collector loops with direct steam generation.* Solar Energy, 2007. 81(2): p. 268-279.
16. Giostri, A., et al., *Comparison of different solar plants based on parabolic trough technology.* Solar Energy, 2012. 86(5): p. 1208-1221.

17. Zarza, E., et al., *Direct steam generation in parabolic troughs: Final results and conclusions of the DISS project.* Energy, 2004. 29(5): p. 635-644.
18. Eck, M., et al., *Applied research concerning the direct steam generation in parabolic troughs.* Solar Energy, 2003. 74(4): p. 341-351.
19. Alguacil, M., et al., *Direct steam generation in parabolic trough collectors.* Energy Procedia, 2014. 49: p. 21-29.
20. Ochoa, L.R., *Engineering Aspects of a Parabolic Trough Collector Field with Direct Steam Generation and an Organic Rankine Cycle.* 2014.
21. *Heat transfer Fluid*. 2015.1.03]; Available from: http://www.solarthermalpowerplant.com/index.php/the-thermal-fluid-htf.
22. Li, J., *Structural Optimization and Experimental Investigation of the Organic Rankine Cycle for Solar Thermal Power Generation*. 2015: Springer.
23. Chaturvedi, S., V. Gagrani, and T. Abdel-Salam, *Solar-assisted heat pump–a sustainable system for low-temperature water heating applications.* Energy Conversion and Management, 2014. 77: p. 550-557.
24. Chaturvedi, S., et al., *Two-stage direct expansion solar-assisted heat pump for high temperature applications.* Applied thermal engineering, 2009. 29(10): p. 2093-2099.
25. Kong, X., et al., *Thermal performance analysis of a direct-expansion solar-assisted heat pump water heater.* Energy, 2011. 36(12): p. 6830-6838.
26. Fernández-Seara, J., et al., *Experimental analysis of a direct expansion solar assisted heat pump with integral storage tank for domestic water heating under zero solar radiation conditions.* Energy Conversion and Management, 2012. 59: p. 1-8.

27. Huang, B. and C. Lee, *Long-term performance of solar-assisted heat pump water heater.* Renewable Energy, 2004. 29(4): p. 633-639.

28. *Solar Assisted Heat Pump – Thermodynamics*. 2015.09.02]; Available from: http://envirosolar.co.uk/little-magic-thermodynamic-box.html.

29. *Multi-function (LCD)Controller solar assisted heat pump*. 2015.09.03.]; Available from: http://www.alibaba.com/product-detail/Multi-function-LCD-Controller-solar-assisted_60132682043.html?spm=a2700.7724857.35.1.FWTRG7.

30. Aljundi, I.H., *Effect of dry hydrocarbons and critical point temperature on the efficiencies of organic Rankine cycle.* Renewable Energy, 2011. 36(4): p. 1196-1202.

31. Saleh, B., et al., *Working fluids for low-temperature organic Rankine cycles.* Energy, 2007. 32(7): p. 1210-1221.

32. Lai, N.A., M. Wendland, and J. Fischer, *Working fluids for high-temperature organic Rankine cycles.* Energy, 2011. 36(1): p. 199-211.

33. Heberle, F. and D. Brüggemann, *Exergy based fluid selection for a geothermal Organic Rankine Cycle for combined heat and power generation.* Applied Thermal Engineering, 2010. 30(11): p. 1326-1332.

34. Liu, B.-T., K.-H. Chien, and C.-C. Wang, *Effect of working fluids on organic Rankine cycle for waste heat recovery.* Energy, 2004. 29(8): p. 1207-1217.

35. He, C., et al., *The optimal evaporation temperature and working fluids for subcritical organic Rankine cycle.* Energy, 2012. 38(1): p. 136-143.

36. Mikielewicz, D. and J. Mikielewicz, *A thermodynamic criterion for selection of working fluid for subcritical and supercritical domestic micro CHP.* Applied Thermal Engineering, 2010. 30(16): p. 2357-2362.

37. *Linuo Paradigma Solar Energy,U-type CPC collectors*. 2015.03.14]; Available from: www.linuo-paradigma.com/chanpinzhongxin/shangyongxilie/tynrsxtsbjc/780.html.
38. Hung, T.-C., T. Shai, and S. Wang, *A review of organic Rankine cycles (ORCs) for the recovery of low-grade waste heat.* Energy, 1997. 22(7): p. 661-667.
39. Roy, J., M. Mishra, and A. Misra, *Parametric optimization and performance analysis of a waste heat recovery system using Organic Rankine Cycle.* Energy, 2010. 35(12): p. 5049-5062.
40. Mago, P.J., et al., *An examination of regenerative organic Rankine cycles using dry fluids.* Applied thermal engineering, 2008. 28(8): p. 998-1007.
41. Roy, J., M. Mishra, and A. Misra, *Performance analysis of an Organic Rankine Cycle with superheating under different heat source temperature conditions.* Applied Energy, 2011. 88(9): p. 2995-3004.
42. Srinivasan, K.K., P.J. Mago, and S.R. Krishnan, *Analysis of exhaust waste heat recovery from a dual fuel low temperature combustion engine using an Organic Rankine Cycle.* Energy, 2010. 35(6): p. 2387-2399.
43. Chen, Q., J. Xu, and H. Chen, *A new design method for Organic Rankine Cycles with constraint of inlet and outlet heat carrier fluid temperatures coupling with the heat source.* Applied Energy, 2012. 98: p. 562-573.
44. Desai, N.B. and S. Bandyopadhyay, *Process integration of organic Rankine cycle.* Energy, 2009. 34(10): p. 1674-1686.
45. *Hi Min Solar*. 2015.03.16]; Available from: http://solarcollectorchina.com/1-3-parabolic-trough-receiver.html.

46. *GE - Model Clean Cycle 125™ - Organic Rankine Cycle (ORC) Systems*. 2015.12.11]; Available from: http://www.environmental-expert.com/products/ge-model-clean-cycle-125-organic-rankine-cycle-orc-systems-177085.

47. *Verdicorp's Organic Rankine Cycle System.* . 2015.11.10]; Available from: http://verdicorp.com/orc.html.

48. *The Motorship - Enertime Organic Rankine Cycle heat recovery technology ready for ships*. 21.12.15]; Available from: http://www.motorship.com/news101/engines-and-propulsion/organic-rankine-cycle-heat-recovery-technology-ready-for-ships.2.

49. Juhasz, J.R. and L.D. Simoni, A review of potential working fluids for low temperature organic Rankine cycles in waste heat recovery. 3rd International Seminar on ORC Power Systems, October 12-14, 2015, Brussels, Belgium, 2015.

50. Molés, F., et al., *Low GWP alternatives to HFC-245fa in Organic Rankine Cycles for low temperature heat recovery: HCFO-1233zd-E and HFO-1336mzz-Z.* Applied Thermal Engineering, 2014. 71(1): p. 204-212.

51. Kontomaris, K., *HFO-1336mzz-Z: High Temperature Chemical Stability and Use as A Working Fluid in Organic Rankine Cycles.* 2014.

52. Raabe, G., *Molecular Simulation Studies on the Vapor–Liquid Equilibria of the cis-and trans-HCFO-1233zd and the cis-and trans-HFO-1336mzz.* Journal of Chemical & Engineering Data, 2015. 60(8): p. 2412-2419.

Figure Captions

Fig.1. The temperature - heat (*T*-*Q*) curve for the evaporator

Fig. 2. Configuration of the proposed solar ORC system

Fig. 3. Influence of critical temperature of working fluid on ORC efficiency

Fig. 4. Influence of critical temperature of working fluid on optimum evaporation temperature

Fig. 5. Influence of critical temperature of working fluid on maximum thermal efficiency

Fig. 6. Influence of critical temperature of working fluid on collector efficiency at evaporation temperature of 120 ^{o}C for solar ORC system with HTF

Fig. 7. Influence of critical temperature of working fluid on on collector efficiency at evaporation temperature of 100 ^{o}C

Fig. 8. Influence of critical temperature of working fluid on collector efficiency at evaporation temperture of 120^{o}C

Fig. 9. Influence of critical temperature of working fluid on collector efficiency at evaporation temperture of 150^{o}C

Fig.10. Influence of critical temperature of working fluid on enthalpy ratio at evaporation temperture of 100,120 and 150^{o}C

Fig. 11. Influence of critical temperature of working fluid on system thermal efficiency at evaporation temperature of 100^{o}C

Fig. 12. Influence of critical temperature of working fluid on system thermal efficiency at evaporation temperature of 120^{o}C

Fig. 13. Influence of critical temperature of working fluid on system thermal efficiency at evaporation temperature of 150^{o}C

Table caption

Table 1 Working fluid properties

Table 2 Relative increment in overall electricity efficiency of solar ORC with DVG

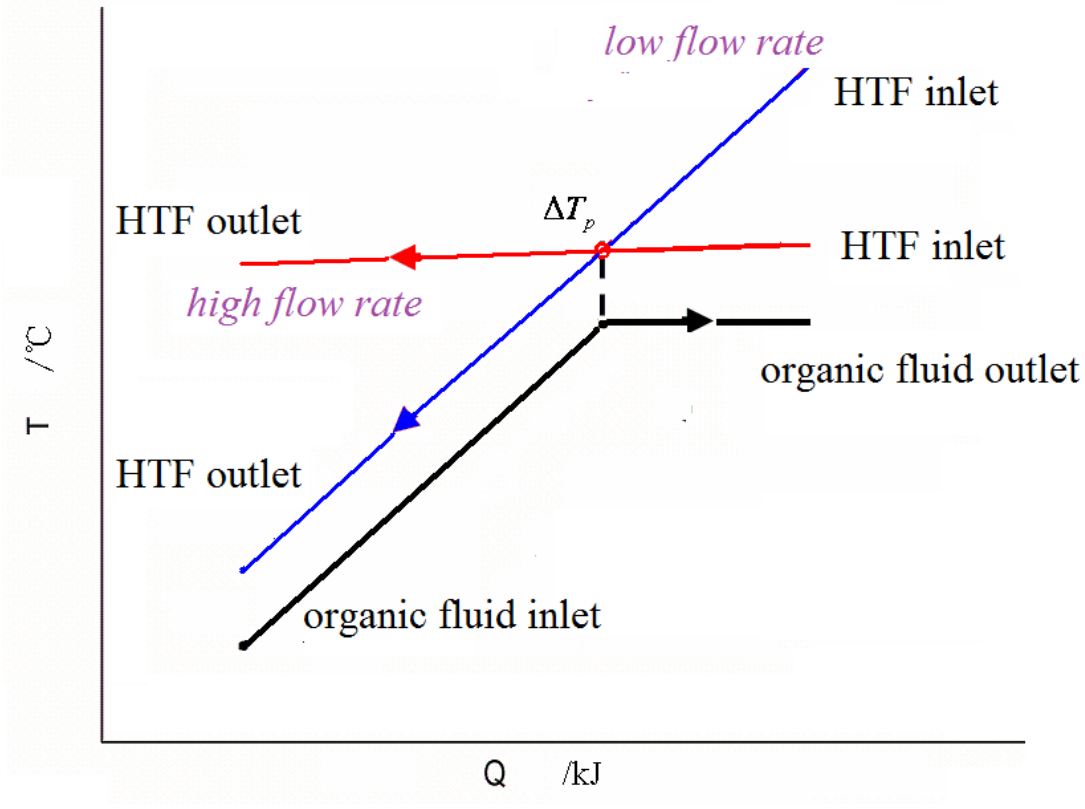

Fig.1. The temperature - heat (*T*-*Q*) curve for the evaporator [22]

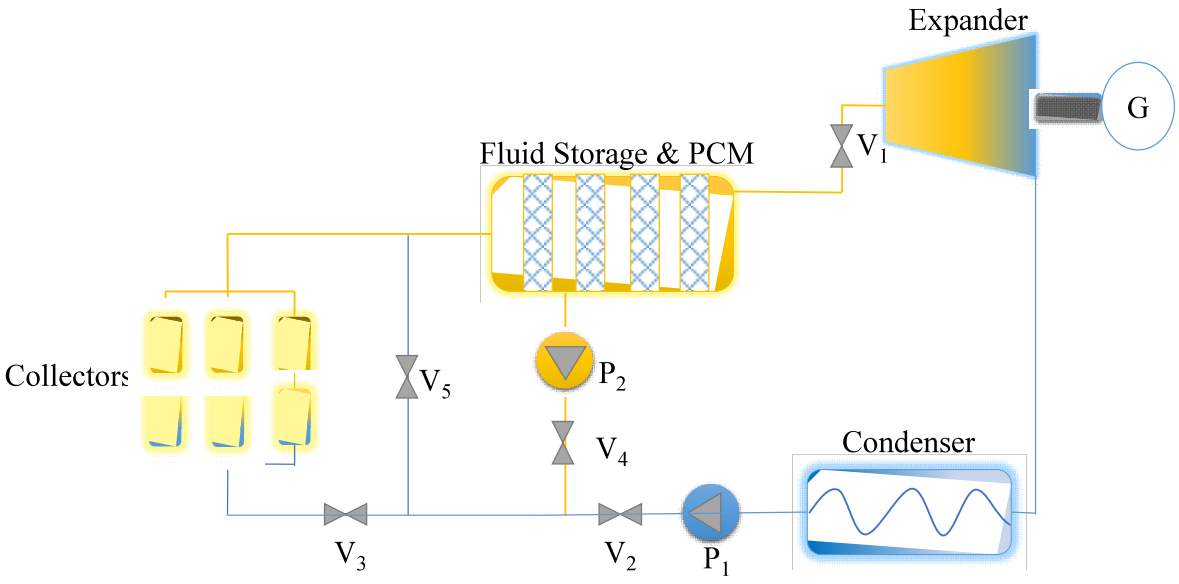

560
561 Fig. 2. Configuration of the proposed solar ORC system

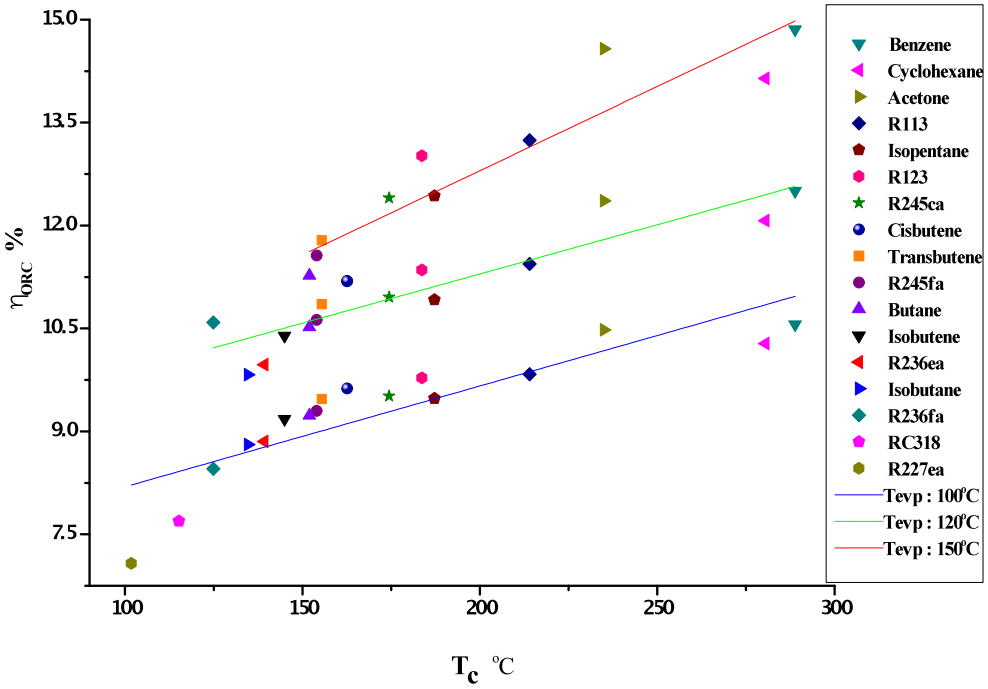

562

563 Fig. 3. Influence of critical temperature of working fluid on ORC efficiency

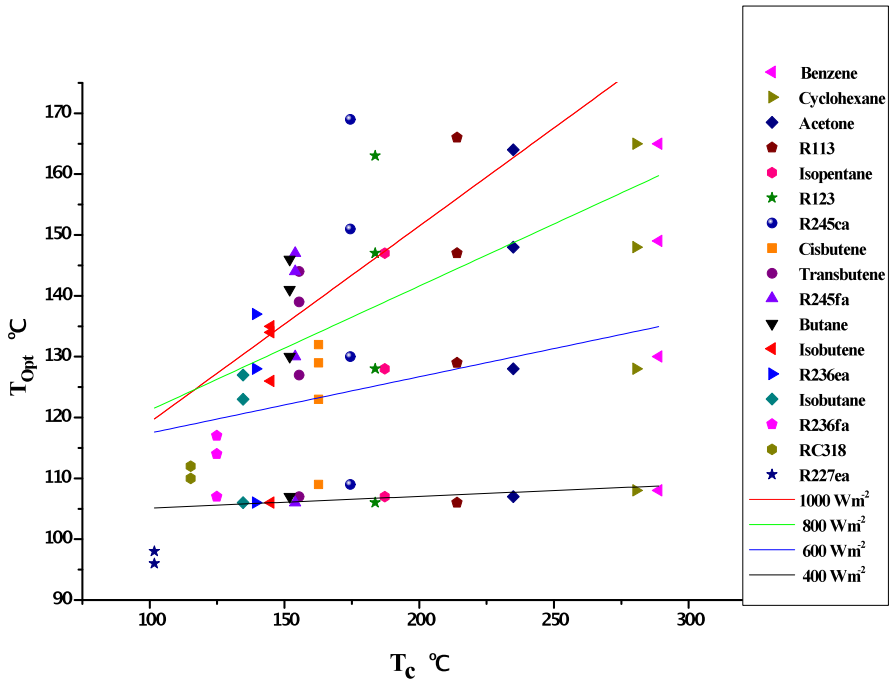

564

565 Fig. 4. Influence of critical temperature of working fluid on optimum evaporation temperature

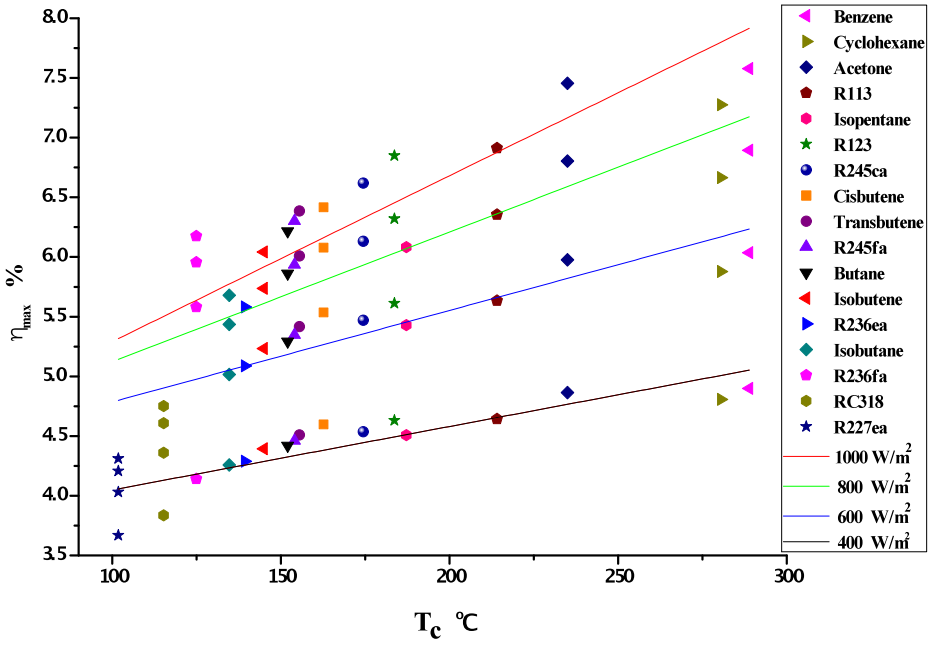

566

567 Fig. 5. Influence of critical temperature of working fluid on maximum thermal efficiency

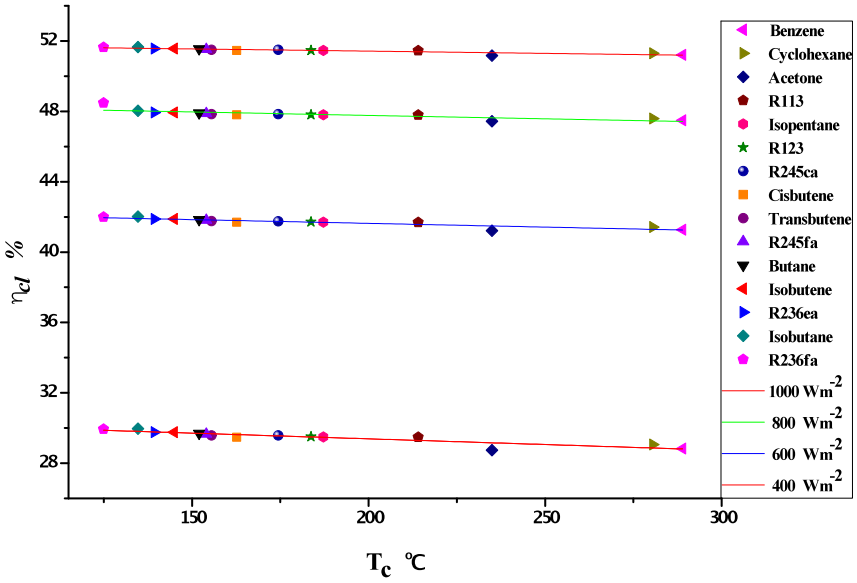

568

569 Fig. 6. Influence of critical temperature of working fluid on collector efficiency at evaporation

570 temperature of 120°C for solar ORC system with HTF

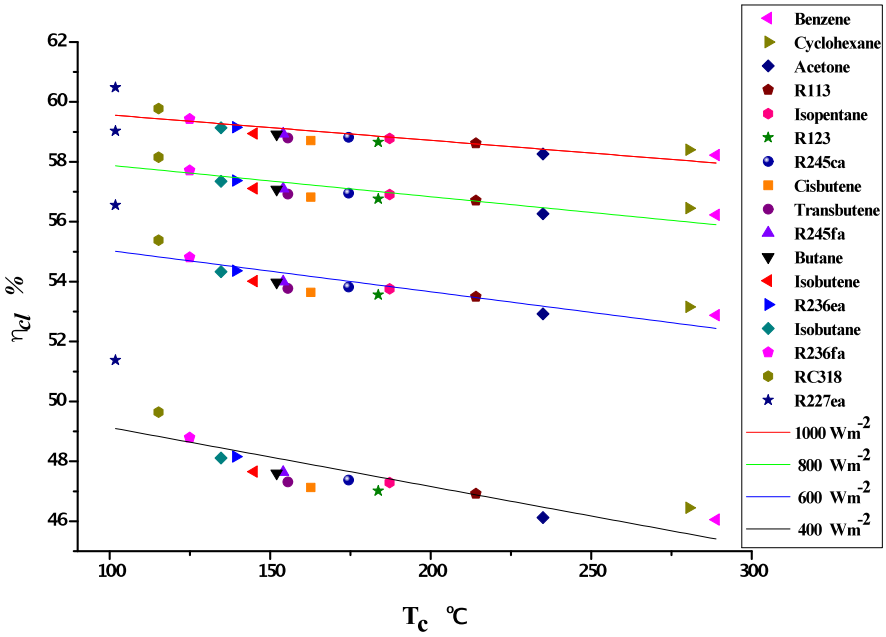

571

572 Fig. 7. Influence of critical temperature of working fluid on on collector efficiency at evaporation

573 temperature of 100°C

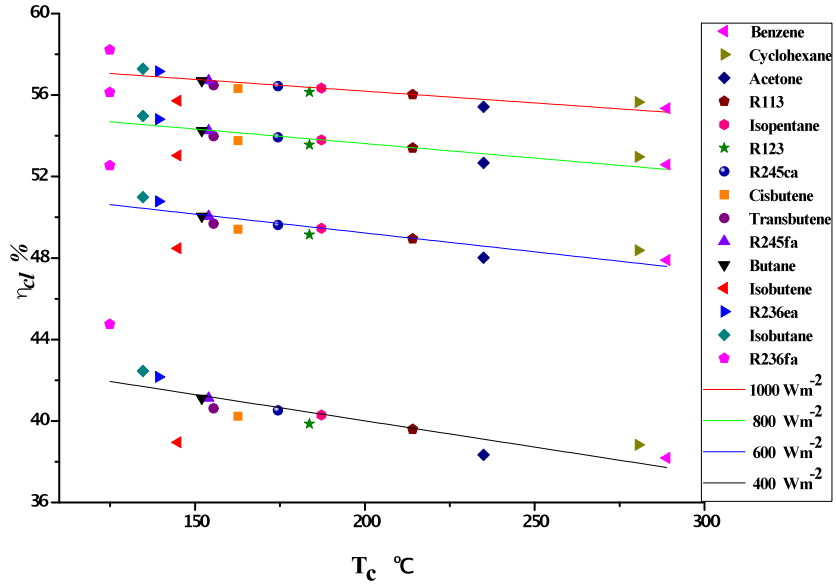

574

575 Fig. 8. Influence of critical temperature of working fluid on collector efficiency at evaporation

576 temperture of 120°C

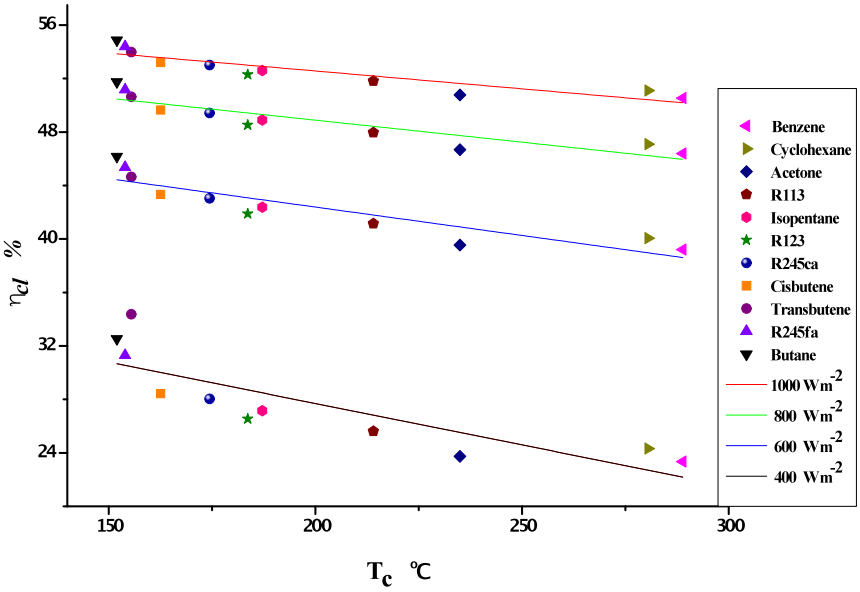

577

578 Fig. 9. Influence of critical temperature of working fluid on collector efficiency at evaporation

579 temperture of 150°C

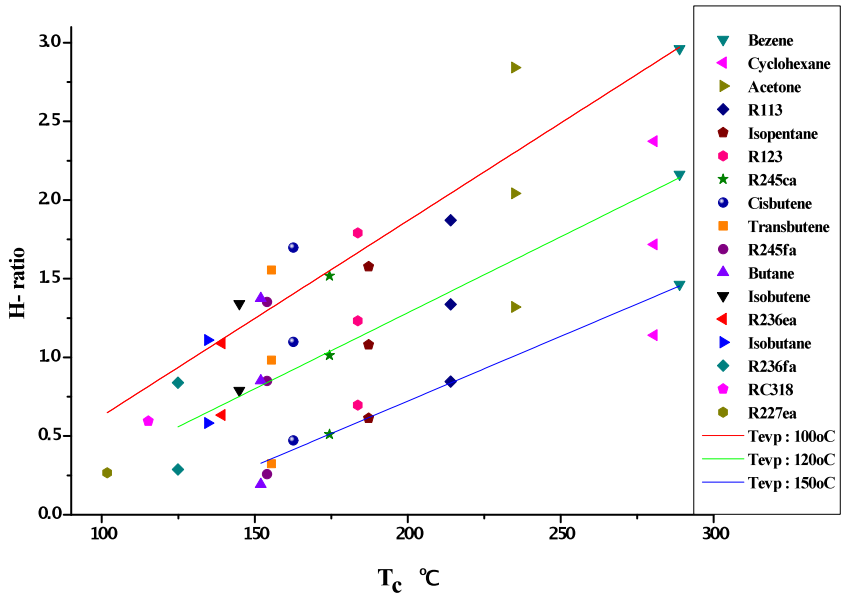

580

581 Fig. 10. Influence of critical temperature of working fluid on enthalpy ratio at evaporation

582 temperture of 100,120 and 150°C

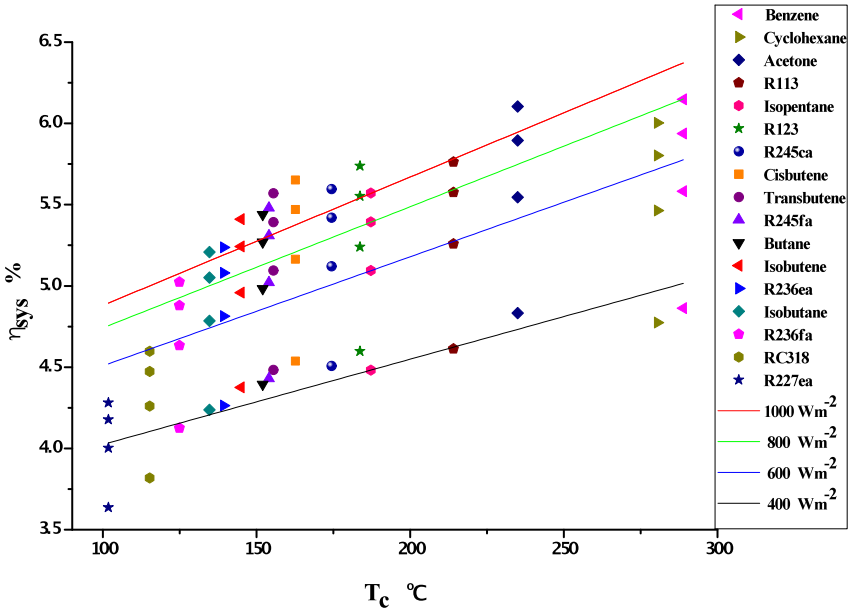

583

584 Fig. 11. Influence of critical temperature of working fluid on system thermal efficiency at

585 evaporation temperature of 100°C

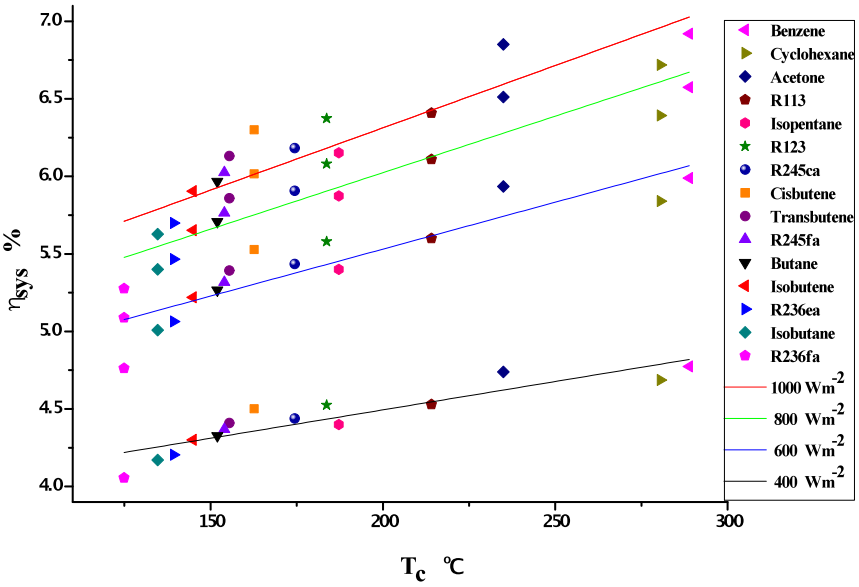

586

587 Fig. 12. Influence of critical temperature of working fluid on system thermal efficiency at

588 evaporation temperature of 120°C

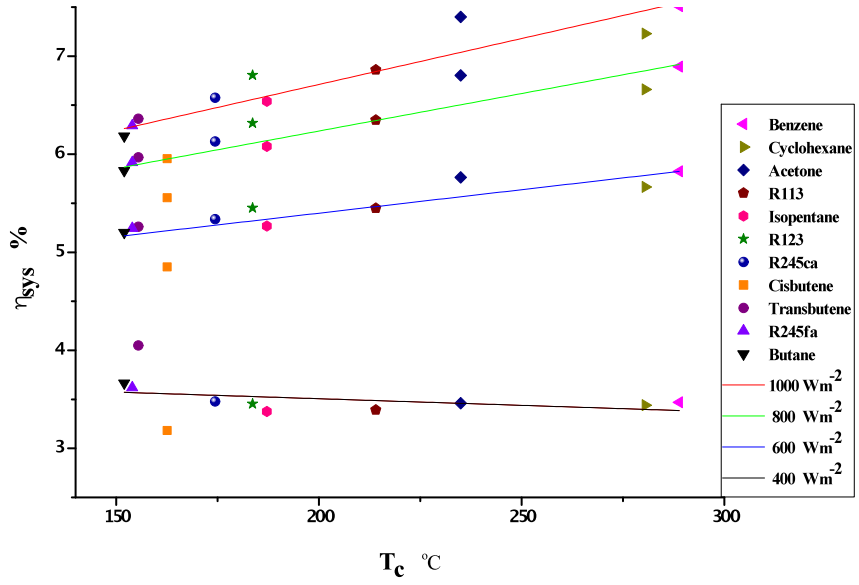

589

590 Fig. 13. Influence of critical temperature of working fluid on system thermal efficiency at

591 evaporation temperature of 150°C

592 Table 1 Working fluid properties

Working fluid	Critical temperature ^{o}C	Critical pressure Mpa	Liquid thermal conductivity at 100^{o}C (mW/m-K)	Semi empirical ODP	Net GWP	Toxicity	Flammability
Benzene	288.9	4.894	-	-	-	high	high
Cyclohexane	280.49	4.075	106.73	-	-	high	high
Acetone	234.95	4.7	-	-	-	low	high
R113	214.06	3.392	53.848	1.0	6130	low	non
Isopentane	187.2	3.378	83.018	0	4± 2	low	extremely
R123	183.68	3.6618	58.190	0.02	77	high	non
R245ca	174.42	3.925	76.127	0	693	-	-
Cis-butene	162.6	4.225	82.893	-	-	non	extremely
Trans-butene	155.46	4.027	81.357	-	-	-	extremely
R245fa	154.01	3.651	64.289	0	1030	low	non
Butane	151.98	3.796	78.234	0	4	low	extremely
Isobutene	144.94	4.009	76.945	0	3	non	extremely
R236ea	139.29	3.502	55.146	0	1370	-	-
Isobutane	134.66	3.629	66.572	0	3	low	extremely
R236fa	124.92	3.2	51.889	0	9810	low	non
R-C318	115.23	2.777	44.883	0	10300	low	non
R227ea	101.75	2.925	48.251	0	3220	low	non

593

594

595

596 Table 2 Relative increment in overall electricity efficiency of solar ORC with DVG, unit: %

Working fluid	Solar radiation			
	400 W/m^2	600 W/m^2	800 W/m^2	1000 W/m^2
Benzene	32.47	16.03	10.53	8.17
Cyclohexane	33.38	16.92	11.21	8.45
Acetone	33.44	16.42	10.86	8.27
R113	34.19	17.38	11.76	8.82
Isopentane	36.63	18.46	12.27	9.52
R123	35.11	17.86	11.97	9.11
R245ca	37.34	18.76	12.69	9.59
Cis-butene	36.40	18.41	12.38	9.40
Trans-butene	37.42	19.03	12.63	9.69
R245fa	38.97	19.75	13.27	10.08
Butane	39.04	19.87	13.21	10.08
Isobutene	31.00	15.68	10.62	8.11
R236ea	41.69	21.25	14.32	10.97
Isobutane	42.05	21.20	14.49	10.89
R236fa	49.63	25.08	15.77	12.76

597

598

599

600

601

602

603

604

605 **Nomenclature (in the sequence of first character of word)**

Symbols		
A	Area, m^2	
c_p	Specific heat, J / kg/ ^oC	
h	Enthalpy, J / kg	
m	Working fluid mass flow rate, kg /s	
Q	Heat transferred, J	
s	Surface area, m^2	
T	Temperature, ^oC	
W	Work done, J	
Abbreviations		
G	Generator	
P	Pump	
V	Valve	
CHP	Combined heat and power	
CPC	Compound parabolic concentrator	
CSP	Concentrated solar power	
DSG	Direct steam generation	
DVG	Direct vapor generation	
ETC	Evacuated tube collector	
FPC	Flat plate collector	
GWP	Global Warming Potential	
HTF	Heat transfer fluid	
ODP	Ozone Depletion Potential	

ORC	Organic Rankine Cycle
PCM	Phase change material
PTC	Parabolic trough concentrator
Subscript	
b	Binary
c	Critical
cl	Collector
evp	Evaporation
g	Generator
i	Inlet
l	Liquid
max	Maximum
o	Outlet
Opt	Optimum
ORC	Organic Rankine Cycle
os	Ideal thermodynamic process
p	Pump
pp	Pinch point
Sys	System
t	Expander
0	Reference state
Greek Symbols	
ε	Mechanical efficiency

Δ	Change
η	Thermal Efficiency
α	Heat capacity coefficient, J / ^{o}C
θ	Arithmetic solution, ^{o}C